Thorium in high-titania slag

by J. Nell*

Transaction Paper

Synopsis

Radioactive elements associated with heavy mineral deposits may be removed from the ilmenite concentrate before smelting or, alternatively, from the high-titanium slag after smelting. Either way, the radioactivity removal process will involve leaching and/or flux-roasting. However, the volume of slag is approximately 50 per cent less than the volume of ilmenite concentrate and it may therefore be more efficient to remove radioactive elements from the slag.

Several slags with different compositions (in terms of iron to titanium ratio, silica content and radio activity) were studied. All the slags contain iron-titanium oxide phases with M_3O_5 ($M = Fe^{2+}$, Ti^{3+}, Ti^{4+}, Mg^{2+}, Al^{2+}, Cr^{3+}) stoichiometry, silicate phases and a small amount of entrained metal droplets. The silicate phases have variable compositions; in all the samples it was found that droplets of a silica-rich phase (containing about 60% SiO_2) unmixes from a low-silica phase (containing about 40% SiO_2). Both the high- and low-silica phases are considered to be glass, representing quenched, immiscible silicate melt phases.

The silicate and oxide phases were analysed by electron microprobe to determine the distribution of thorium in the slag (the concentrations of the radioactive daughter products of the thorium decay series are too low to be detected with the microbeam analytical facilities that were available during the investigation). The results are unequivocal: the concentration of thorium in M_3O_5 oxide phases is below the detection limit of the technique (500 ppm) while the concentration in the silicate phases is at the one per cent level. Furthermore, the concentration of thorium in the low-silica phase (which also contains high concentrations of Zr and Ce) is considerably higher than in the high-silica phase. Mass-balance calculations indicate that the slags contain about 5 per cent by weight silicate phases and that the amount of thorium present in silicate phases is enough to account for the total thorium content of the slags.

There is firm evidence for the concentration of thorium in silicate phases but the distribution of the radioactive daughter elements of the thorium and uranium decay series could not be determined directly. To obtain more information on the distribution of trace elements in high-titanium slag, proton induced X-ray emission spectroscopy (PIXE) was used to characterize, semi-quantitatively, the distribution of elements between coexisting silicate- and oxide-phases in one of the samples. The results confirmed the partitioning of thorium to silicate phases. In addition, it was found that the low-silica phase, which contains most of the thorium, is also enriched in Zr, Ce, Nb, Ta, Ba, Y, U and Sr. Elements with large ionic radii are apparently concentrated in the low-silica phase; it is expected that the daughter products of the Th- and U-decay series would behave similarly.

Therefore, to lower the radioactivity, the silicate phases must be removed from the slag. One way to do so is to subject the slag to NaOH leaching, followed by acid leaching. Another approach would be to use a modified SREP method but this runs the risk of contaminating the final slag product with impurities such as boron.

Introduction

Heavy mineral deposits often contain relatively high levels of radioactive elements (thorium and uranium in particular). It is difficult to obtain clean separation of ilmenite and monazite (the main impurity mineral containing radioactive elements), and physical intergrowths of the two minerals are, in fact, not uncommon. As a result, ilmenite concentrates obtained from such deposits often contain high levels of thorium and uranium. Because of the large negative free energies of formation of ThO_2 and U_3O_8 both thorium and uranium report to the slag during smelting and if an ilmenite concentrate contaminated with monazite is used to make high titania slag, the concentrations of these elements in the slag end up about 40% higher than in the ilmenite feed.

Previous work, patented by RGC Mineral Sands Limited, and subsequently confirmed by Mintek, showed that radioactivity may be reduced by roasting an ilmenite concentrate with borax at 1000°C to 1100°C and leaching it with hydrochloric acid[1]. It is evident that the cost of an ilmenite roast/leach process will be high and there may be economic benefits in removing the radioactive elements from the slag instead (the volume of slag to be treated is smaller than the volume of ilmenite feed).

To remove radioactive elements from the slag it is necessary to know how these elements occur in the slag. In other words, the distribution of uranium and thorium between the various oxide, silicate and metallic phases in high titania slag must be determined. Once the deportment of thorium and uranium between the various phases has been determined, an appropriate process for slag purification can be developed.

Test samples

High-titania slag was prepared in a pilot-scale DC furnace from ilmenite concentrates with different levels of uranium and thorium. Subsequently, ten slag samples representing a

* *Mintek, Randburg, South Africa, (now at Hatch).*

 SA ISSN 0038–223X/3.00 + 0.00. This paper was first published at the SAIMM Conference, Heavy Minerals, *10–14 September 2007*

range of compositions were selected for bulk chemical analysis, scanning electron microscopy and micro-analysis. The samples were crushed to a maximum particle size of 1 mm and from each sample a 20-kg batch was riffled out for analysis.

Bulk chemical composition

Chemical compositions of the samples selected for test work are given in Table I. TiO_2, Al_2O_3, SiO_2, MgO, MnO, FeO and V_2O_5 were analysed by ICP-OES, Na_2O, CaO and Cr_2O_3 by atomic absorption spectroscopy and U and Th by XRF (the XRF detection limit for U and Th was around 4 ppm). The 'B' series has a higher silica content than the others as a result of small silica additions that were made during smelting. All samples have elevated alumina levels as a result of furnace refractory contamination during smelting.

As expected, there is an inverse relationship between the concentrations of TiO_2 and FeO in the samples (Figure 1). The TiO_2 and FeO levels are similar to the levels found in industrial slags[2]. Extreme conditions of reduction under which reduction of more 'refractory' oxides (e.g., chromia, magnesia, silica, alumina and even urania and thoria) might take place were not explored in the study. Note that BB1 and BBB1 contain more than 7% combined silica and alumina (SiO_2 as a flux addition during smelting, and Al_2O_3 from refractory contamination) and they do not fall on the general trend defined by the other samples.

The U and Th concentrations of sample E2 is noteworthy. In the preparation of slag E2, monazite concentrate was added to the ilmenite to increase the concentrations of radioactive elements in the slag. This was done primarily to facilitate the detection of Th and U during the phase chemical characterization of the slag.

Radioactivity measurements

Gamma ray emissions from the samples were measured with a gamma ray detector. Measurements were performed on 50-g samples, counting for 400 seconds. Repeated measurements (between 3 and 6) were performed on each sample to calculate mean values and standard deviations (Table II). There is good agreement between gamma ray emissions and the combined thorium and uranium concentrations of the samples (Figure 2). A regression of the data gives:

$$U + Th\ (\text{in ppm}) = -5.4 + (1020.0) * (NC) \quad [1]$$

where NC is the normalized gamma-ray emission in units of counts.gram^{-1}.seconds^{-1}. It is important to note that Equation [1] is strictly valid for the slag samples that were analysed and that it cannot be applied to other materials.

Reconciliation of the radioactivity of the slags with the concentrations of radioactive elements was not undertaken. There can be no doubt that the radioactive decay series in the slags are not in equilibrium owing to factors such as the volatilization of some of the daughter elements during smelting.

Phase-chemical characterization of the slag

X-ray diffractometry

Powder X-ray diffraction was used to identify the phases present in the samples. In all the samples, the most abundant phase belongs to the M_3O_5 multi-component solid-solution series (in high-titanium slags *M* may be Ti^{4+}, Ti^{3+}, Fe^{2+}, Mg^{2+} and Al^{3+}, appropriately combined to maintain charge balance in the structure). All the slags contain TiO_2 (rutile) in trace amounts.

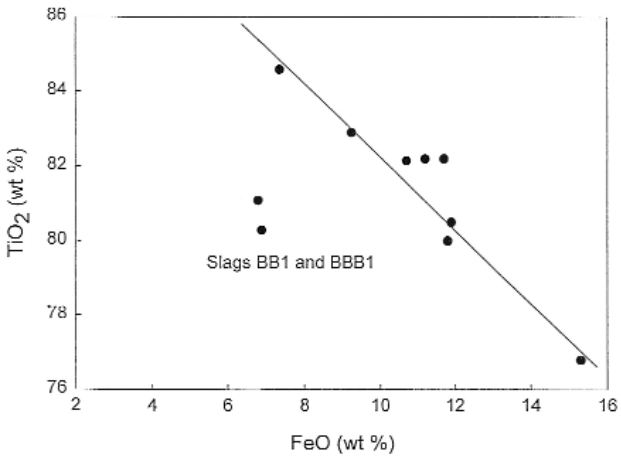

Figure 1—Relationship between the TiO_2 and FeO concentrations in the selected slags

Table I

Bulk chemical compositions of the slag samples selected for test purposes

	A1	A6	A12	B4	BB1	BBB1	E2	F3	G3	H4
TiO_2	84.6	80.5	76.8	82.9	81.1	80.3	80.0	82.2	82.2	82.15
FeO	7.35	11.9	15.3	9.24	6.79	6.88	11.8	11.2	11.7	10.7
CaO	0.15	0.10	0.11	0.08	0.14	0.13	0.09	0.06	0.06	0.11
MgO	1.65	1.33	1.43	1.37	1.90	1.90	1.28	0.77	1.26	1.41
MnO	1.82	1.67	1.65	1.64	1.87	1.86	1.69	1.78	1.70	1.91
SiO_2	2.12	1.76	1.82	2.19	3.30	3.30	1.86	1.75	1.37	1.81
Al_2O_3	2.59	2.09	2.31	2.03	3.88	3.83	2.09	1.86	1.45	1.89
Cr_2O^3	0.46	0.41	0.40	0.42	0.39	0.38	0.43	0.33	0.44	0.42
V_2O_5	0.33	0.32	0.32	0.33	0.30	0.30	0.32	0.28	0.32	0.33
Na_2O	0.05	0.05	0.05	0.04	0.07	0.08	0.05	0.04	0.02	0.06
Total	**101.1**	**100.13**	**100.19**	**100.24**	**99.73**	**98.96**	**99.61**	**100.28**	**100.52**	**100.79**
Th	139	182	161	177	203	173	336	220	177	50
U	11	20	12	19	17	16	14	0	20	8

Table II

Gamma-ray emissions from samples selected for test-work. Results are expressed as (counts. second^{-1}.gram^{-1}), standard deviations are given in parentheses

Sample	Normalized gamma-ray counts
A1	0.183 (0.002)
A6	0.187 (0.001)
A12	0.187 (0.003)
B4	0.199 (0.001)
BB1	0.215 (0.001)
BBB1	0.217 (0.002)
E2	0.341 (0.004)
F3	0.204 (0.001)
G3	0.188 (0.002)
H4	0.056 (0.001)

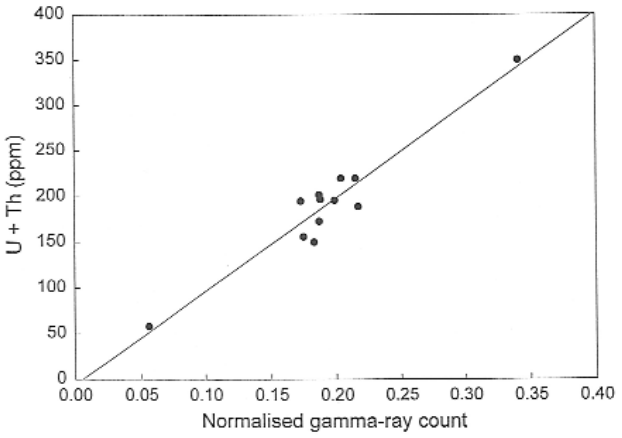

Figure 2—Gamma ray emissions from the samples as a function of the combined uranium and thorium concentrations

The shape of the background at small diffraction angles indicates the presence of small amounts of silicate glass in the slags. This feature was particularly prominent in the 'B' series of samples and is consistent with the addition, during smelting, of SiO_2 to these samples.

Micro-analysis

The slags, after tapping, consist mostly of iron-titanium oxides (M_3O_5 solid solutions where M = Ti^{4+}, Ti^{3+}, Fe^{2+}, Mg^{2+}, Mn^{2+} and Al^{3+}) and silicate phases. The aim of this part of the characterization is to determine how the radioactive elements are distributed between these phases. This information is critical to develop methods for the removal of impurities from the slag.

Proton induced X-ray emission spectroscopy (PIXE)

Measurements on slag F3, which was doped with monazite, were performed by iThemba Laboratories. The advantage offered by PIXE is a relatively low detection limit for elements with high atomic mass, such as thorium and uranium. However, there are also drawbacks to the technique:

- The inability to analyse elements with an atomic number below about 20 (Ca) when these are contained in phases with a high mean atomic number
- The semi-quantitative nature of the analyses (measurements are standardless, although matrix corrections are performed).

It is therefore not possible to perform comprehensive, quantitative chemical analyses of the phases present in the slag using this technique.

However, the instrument can be used to generate concentration maps for areas of slag measuring almost 0.5 mm^2. This provides a powerful visual image of the distribution of trace elements between the coexisting phases over a relatively large area of slag. Such maps for a grain of slag consisting of silicate and oxide phases are shown in Figure 3 and Figure 4. In Figure 3 the silicate phases are characterized by high concentrations of iron and manganese and a relatively low titanium content. The observations may be summarized as follows:

- All the trace-elements detected by the instrument (Th, U, Y, Zr, Nb, Ta, Ba and Ce) partition preferentially into silicate phases (Figure 4)
- Some of the elements, such as Th, Zr, Nb and Ta, are uniformly distributed throughout the silicate phases while others such as U, La and Ba are concentrated in localized regions within silicate grains.

The partitioning of Th, U, Y, Zr, Nb, Ta, Ba and Ce into silicate phases is noteworthy. These elements have large atomic masses and large ionic radii. This is also a characteristic of the radioactive daughter elements generated by the decay series of thorium and uranium. By implication these elements should also concentrate in the silicate phases, rather than in the oxide phases present in the slag.

The PIXE data for chromium are more ambiguous. Several grains of slag containing silicate and oxide phases were mapped; in one instance chromium showed a slight preference for silicate phases but in other cases the distribution was more uniform. Microprobe data (see below) are in agreement with the latter scenario, indicating a slight preference of chromium for M_3O_5 oxide phases.

The thorium content of the silicate phases was found to be approximately 4 500 ppm. This means that the thorium content of the titanium oxide phases must be below 220 ppm (the bulk thorium content of the sample). This constrains the distribution coefficient for thorium between silicate and oxide phases ($D_{Th}^{Silicate-oxide}$ = wt% Th in silicate/wt% Th in oxide) to be greater than 20. The approximate uranium content of the silicate phases is about 100 ppm but the distribution coefficient could unfortunately not be estimated because the uranium content of the bulk sample was below the detection limit of the measurement technique.

Electron microprobe analysis

Electron microprobe analysis using wavelength dispersive X-ray spectroscopy (WDS) was performed to quantify the thorium content of the silicate phases present in each of the samples (the uranium concentration in the silicate phases was similar to the detection limit and it was not measured). The detection limit for thorium is about 500 ppm (for a counting time of 300 seconds), well below the concentration level in the silicate phases, but above the concentration in

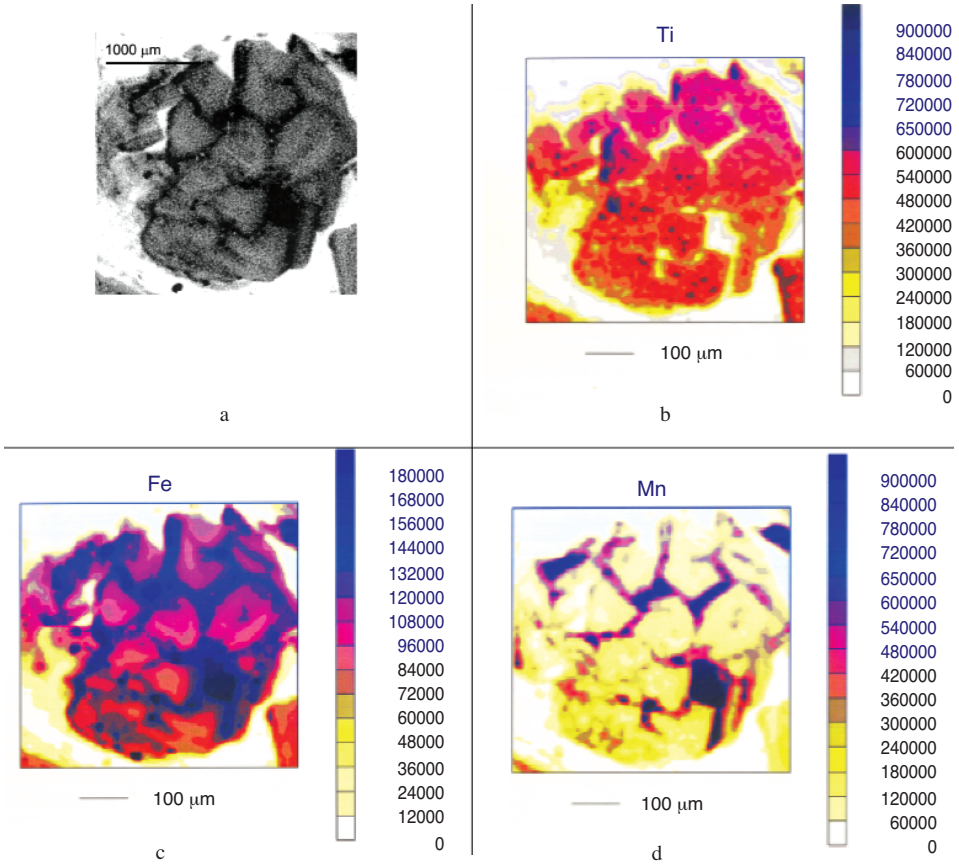

Figure 3—Backscattered electron image (a) and distribution maps of titanium (b), iron (c) and manganese (d), to illustrate the location of silicate and oxide phases in a fragment of slag from sample F3. In the backscattered electron image the silicate phases are black in colour and the titanium oxides are grey. Elemental maps were composed using the PIXE facility at iThemba Laboratories

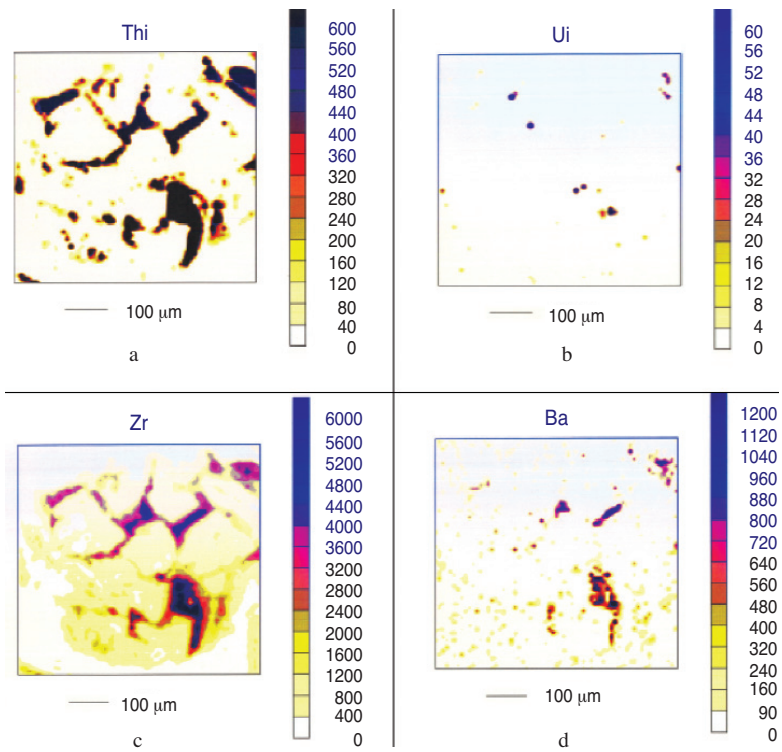

Figure 4—Elemental maps of thorium (a), uranium (b), zirconium (c) and barium (d) in silicate and titanium oxide phases in the grains shown in Figure 3. Maps were composed using the PIXE facility at iThemba Laboratories

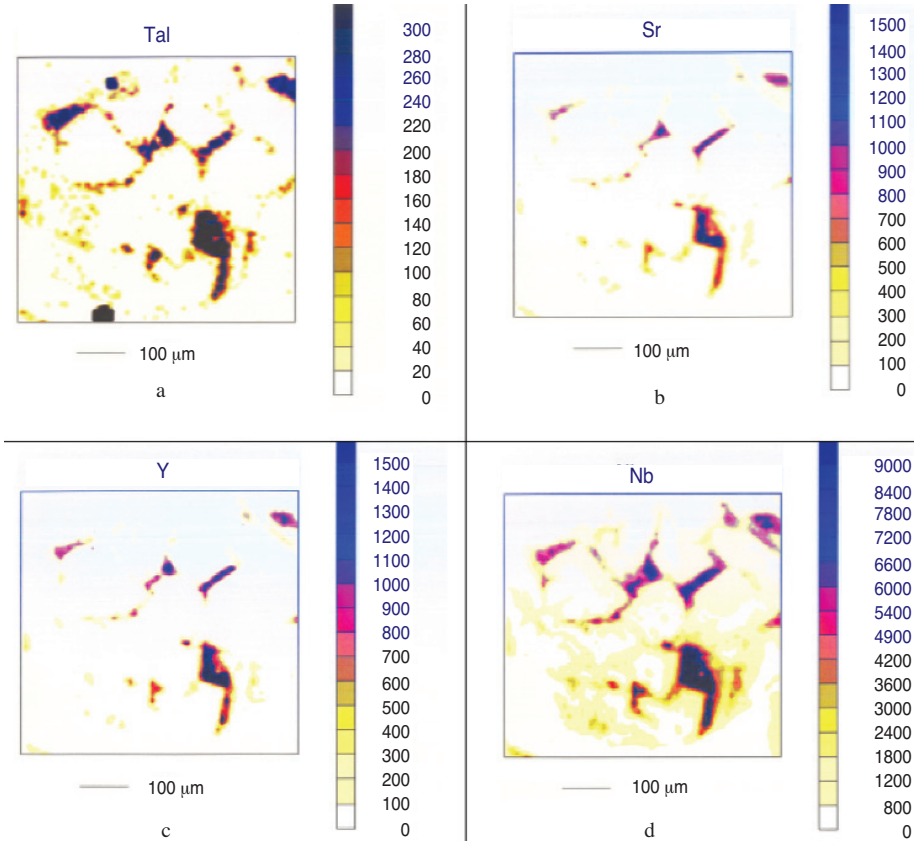

Figure 4 (continued)—Elemental maps of tantalum (a), strontium (b), yttrium (c) and niobium (d) in silicate and titanium oxide phases in the grains shown in Figure 3

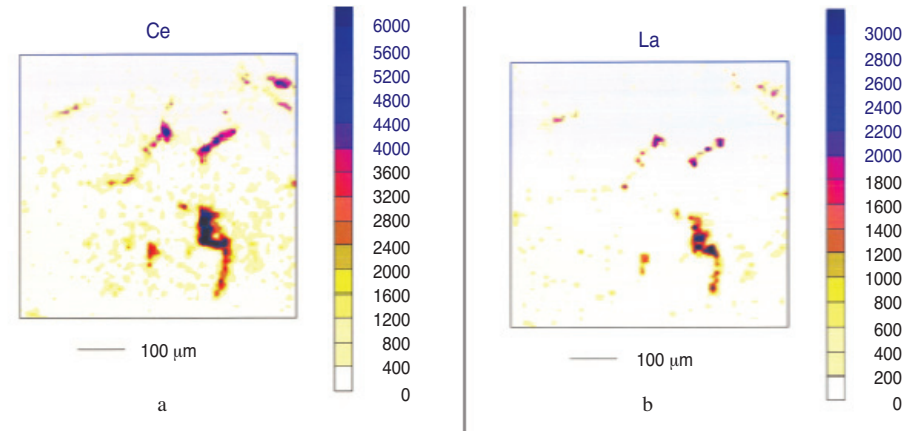

Figure 4 (continued)—Elemental maps of cerium (a) and lanthanum (b) in silicate and titanium oxide phases in the grains shown in Figure 3

M_3O_5 titanium-oxide phases. The thorium content of the latter phases could therefore not be measured.

With rare exceptions, between 5 and 10 points of each phase were analysed per sample. Mean values and standard deviations for silicate and oxide phases are reported in Table III and Table IV respectively. Several factors may contribute to the low analytical totals obtained for some of the analyses:

- The presence of sulphur (up to about 4% by weight in extreme cases), potassium (maximum of about 1% by weight), and other trace elements such as niobium in the silicate phases. To include these elements would have extended counting times well beyond 5 minutes per analysis; this was considered to be counter-productive in terms of the objectives of the work
- The volatilization of sodium during analysis
- Complicated interelement correction procedures due to the high thorium and zirconium concentrations in the phases.

In most slags more than one type of silicate could be identified on the basis of the concentrations of SiO_2, MnO

Table III

Electron microprobe analyses of silicate phases in the slag samples (standard deviations are given in parentheses)

Sample	ZrO_2	ThO_2	MnO	Na_2O	MgO	Al_2O_3	FeO	SiO_2	TiO_2	Cr_2O_3	CaO	Total
A1: 1	2.10 (0.20)	0.41 (0.05)	16.13 (2.87)	0.53 (0.08)	1.17 (0.05)	10.19 (0.29)	5.95 (1.06)	44.97 (2.93)	8.68 (0.84)	0.25 (0.03)	4.61 (0.15)	94.99
A1: 2	1.84 (0.44)	0.43 (0.07)	9.90 (2.35)	0.59 (0.24)	0.91 (0.14)	11.21 (1.27)	3.51 (1.01)	53.74 (2.46)	7.26 (0.55)	0.16 (0.04)	4.60 (0.74)	94.15
A6: 1	1.88	0.65	19.64	0.40	0.80	6.52	18.43	35.09	6.61	0.13	3.22	93.37
A6: 2	1.14 (0.10)	0.44 (0.31)	5.22 (1.52)	1.07 (0.31)	0.44 (0.10)	10.04 (0.24)	3.42 (0.55)	53.71 (0.18)	14.06 (0.71)	0.12 (0.01)	3.11 (0.53)	92.77
A6: 3	0.84 (0.20)	0.23 (0.09)	4.66 (1.09)	0.81 (0.20)	0.34 (0.06)	10.69 (0.51)	3.56 (1.03)	65.97 (1.56)	6.15 (0.40)	0.06 (0.01)	2.99 (0.61)	96.30
A12: 1	1.50 (0.21)	0.55 (0.09)	15.38 (1.28)	0.45 (0.10)	1.08 (0.17)	8.03 (0.34)	17.29 (2.54)	36.52 (0.73)	7.63 (0.93)	0.12 (0.02)	3.06 (0.38)	91.61
A12: 2	0.94 (0.04)	0.32 (0.03)	7.43 (2.59)	0.63 (0.29)	0.55 (0.20)	10.83 (1.16)	7.39 (2.87)	57.45 (4.23)	4.86 (0.34)	0.06 (0.02)	2.69 (0.15)	93.15
A12: 3	2.07 (0.24)	0.65 (0.09)	4.94 (1.40)	0.59 (0.33)	0.55 (0.14)	12.61 (0.62)	10.04 (1.29)	50.08 (1.54)	7.89 (3.12)	0.12 (0.04)	3.52 (0.45)	93.06
B4	0.53 (0.09)	0.09 (0.02)	4.38 (1.03)	0.70 (0.37)	0.33 (0.04)	8.39 (0.38)	2.90 (0.41)	73.26 (1.64)	6.85 (0.84)	0.07 (0.02)	1.78 (0.29)	99.28
BB1: 1	1.57 (0.15)	0.34 (0.03)	13.28 (1.07)	0.78 (0.09)	2.13 (0.14)	14.07 (0.63)	7.76 (1.37)	47.46 (1.89)	6.49 (0.77)	0.23 (0.03)	2.54 (0.09)	96.65
BB1: 2	1.36	0.34	9.72	0.99	1.59	15.97	3.92	56.12	4.81	0.12	2.69	97.63
BBB1: 1	1.52 (0.13)	0.33 (0.02)	13.64 (0.55)	0.71 (0.07)	2.58 (0.04)	14.55 (0.26)	7.16 (0.77)	47.40 (0.82)	6.29 (0.89)	0.32 (0.08)	2.51 (0.06)	97.01
BBB1: 2	1.31 (0.16)	0.26 (0.03)	9.54 (1.59)	1.03 (0.08)	1.82 (0.12)	14.27 (0.21)	3.22 (0.25)	51.30 (0.41)	13.17 (1.82)	0.21 (0.02)	2.43 (0.02)	98.56
E2: 1*	n.d. (0.26)	1.20 (2.04)	n.d. (2.32)	n.d. (2.67)	n.d. (0.30)	n.d.	12.86	34.07	11.09	n.d.	3.05	62.27
E2:2	0.75 (0.28)	0.18 (0.05)	3.84 (0.94)	0.80 (0.22)	0.27 (0.07)	10.34 (0.33)	3.77 (1.24)	69.57 (0.67)	6.32 (0.92)	0.06 (0.02)	1.93 (0.42)	97.83
F3	0.37 (0.05)	0.11 (0.04)	3.52 (0.85)	0.74 (0.23)	0.12 (0.02)	9.02 (0.45)	3.16 (0.56)	73.25 (2.15)	7.41 (2.24)	0.05 (0.01)	1.71 (0.25)	99.46
G3	0.37 (0.11)	0.04 (0.02)	2.76 (0.71)	0.61 (0.05)	0.16 (0.02)	7.55 (0.26)	2.88 (0.41)	77.40 (1.36)	6.17 (1.06)	0.04 (0.01)	1.50 (0.23)	99.48
H4:1	1.75 (0.60)	0.13 (0.07)	16.41 (8.71)	1.10 (0.69)	1.07 (0.35)	7.70 (1.01)	9.46 (2.73)	41.62 (4.65)	15.12 (10.25)	0.35 (0.23)	3.40 (1.81)	98.11
H4: 2	0.67 (0.13)	0.06 (0.03)	6.15 (1.55)	1.07 (0.52)	0.43 (0.09)	9.65 (0.65)	4.19 (0.97)	66.14 (2.68)	6.64 (1.45)	0.07 (0.01)	2.60 (1.00)	97.67

*Analyses of the silica-poor phase in E2 are incomplete due to instrumental difficulties at the time of analysis

Table IV

Electron microprobe analyses of iron-titanium oxide phases in the slag samples (standard deviations are given in parentheses)

Sample	ZrO_2	MnO	MgO	Al_2O_3	FeO	SiO_2	TiO_2	Cr_2O_3	CaO	Total
A1	0.16 (0.10)	1.34 (1.10)	1.78 (0.03)	3.22 (0.07)	6.11 (0.65)	0.07 (0.04)	91.06 (2.91)	0.45 (0.10)	0.02 (0.01)	104.21
A6	0.15 (0.11)	1.60 (0.57)	1.55 (0.16)	2.70 (0.19)	10.74 (0.91)	0.04 (0.04)	85.19 (3.24)	0.45 (0.06)	0.01 (0.01)	102.43
A12	0.21 (0.16)	1.35 (0.61)	1.63 (0.31)	2.99 (0.21)	13.39 (3.10)	0.04 (0.02)	83.51 (3.21)	0.51 (0.09)	0.01 (0.01)	103.64
B4	0.18 (0.09)	0.99 (0.70)	1.54 (0.12)	2.64 (0.16)	8.24 (1.98)	0.05 (0.02)	90.32 (2.77)	0.46 (0.10)	0.01 (0.01)	104.43
BB1	0.24 (0.18)	1.36 (0.65)	2.15 (0.08)	4.52 (0.14)	5.67 (1.78)	0.05 (0.03)	90.38 (3.12)	0.43 (0.14)	0.02 (0.01)	104.82
BBB1	0.19 (0.06)	1.17 (0.38)	1.92 (0.30)	3.94 (1.08)	6.79 (2.82)	0.05 (0.02)	89.47 (3.57)	0.41 (0.11)	0.01 (0.01)	103.95
E2	0.43 (0.20)	1.68 (0.88)	1.38 (0.18)	2.69 (0.19)	11.51 (1.89)	0.07 (0.03)	86.01 (3.39)	0.58 (0.12)	0.01 (0.01)	104.36
F3	0.09 (0.05)	0.78 (0.61)	1.03 (0.04)	2.51 (0.11)	6.87 (1.03)	0.02 (0.01)	93.97 (0.78)	0.26 (0.02)	0.00	105.53
G3	0.25 (0.03)	1.15 (0.32)	1.55 (0.05)	2.07 (0.04)	9.16 (0.48)	0.02 (0.01)	90.21 (1.08)	0.49 (0.03)	0.00	104.90
H4	0.16 (0.11)	1.45 (0.81)	1.65 (0.19)	2.49 (0.13)	9.35 (2.22)	0.04 (0.02)	89.04 (2.99)	0.47 (0.11)	0.01 (0.01)	104.66

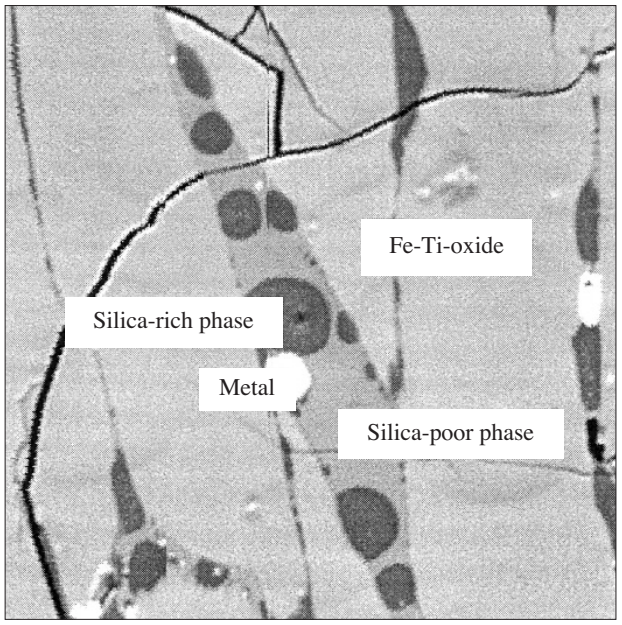

Figure 5—Backscattered electron image illustrating textural relationships between different silicate phases in slag H4. Droplets of a silica-rich phase are surrounded by a silica-poor phase

and FeO. The silicate phases are characterized by complex chemical compositions and a lack of crystalline textures, i.e., they have the chemical and morphological characteristics of glass. The presence of silicate glass in the samples is consistent with the presence of amorphous material detected by XRD. The glass represents silicate melt that coexists with the titanium oxide melt at furnace operating temperatures.

Silica-poor glass is characterized by high concentrations of FeO and MnO. There is also a positive correlation between the concentrations of MnO and FeO in the silica-poor glass. Texturally, silica-rich glass occurrs as rounded droplets within the silica-poor glass (Figure 5), suggesting immiscibility of two silicate melts at high temperatures. The ThO_2 and ZrO_2 concentrations in the different silicate phases in a particular slag are inversely proportional to the silica content, i.e., thorium and zirconium partition preferentially to the silica-poor glass. These relationships are illustrated by the data for samples E2 and H4 in Table IIII (owing to the poor optical imaging on the instrument used for the WDS analysis it was not possible to distinguish between different silicate phases in the slag. Consequently, no analyses of the silica-poor phase were obtained for B4, F3 and G3).

The high thorium content of the silicate phases is one of the most important observations of this study. It is important to note that the concentration levels of thorium in silica-poor glasses are still well below the values at which silicate melts (glasses) become saturated with thorium. High alkali-borosilicate glasses quenched from 1250°C contain between 2% and 5% Th (2.3%–5.7% ThO_2 by weight) in solution[3]; data cited by Farges 4 suggest similar solubility levels in alumino-silicate glasses quenched from the same temperature. He also noted an increase in the solubility of thorium with increasing temperature. The silicate glasses in the high-titanium slags are therefore not expected to be saturated in thorium (the reason for the difference in thorium content of the different silicate glasses will be discussed in a later section).

The distribution of thorium between silicate and oxide-phases will be reported later; as an initial observation it is sufficient to note that thorium has a strong preference for silicate phases.

The oxide phases contain MgO in quantities similar to those present in the coexisting silicate phase but virtually no CaO. To the extent that this signifies a tendency for alkali earth metals with large ionic radii to partition into silicate phases, this is highly significant (such a tendency is in agreement with the PIXE results that show preferential partitioning of barium to the silicate phases). Radium, an alkali earth metal considered to be an important source of radioactivity in slag, has an ionic radius of 1.40 Å, much larger than the radii of Ba^{2+} and Ca^{2+} (1.35 Å and 0.99 Å respectively). The observed partitioning behaviour of MgO, CaO and BaO suggests that RaO also will partition to the silicate phases present in the slag, but even more so than the lighter alkali earth metals.

Distribution of elements between silicate and oxide phases

The distribution of elements between silicate and oxide-phases is a reflection of the thermodynamic behaviour of the system. The distribution coefficient for element *i*, D_i, is defined as:

$$D_i = wt\% \text{ in silicate phases} / wt\% \ i \text{ in oxide phases} \quad [2]$$

The value of D_i, depends on variables such as temperature, oxygen partial pressure (i.e., slag-grade) and melt composition. If there is a sufficient dependence on melt composition it would, in principle, be possible to manipulate the behaviour of impurities during smelting. In the context of this study it would be highly desirable to calculate D_{Th} for each of the slags. Due to the low concentration of thorium in the oxide phases it was unfortunately not possible to measure D_{Th} directly, although minimum values were estimated from mass-balance constraints.

Compositional data for silicate- and oxide-phases were used to calculate D_{Mn}, D_{Mg}, D_{Al}, D_{Fe}, D_{Ti} and D_{Cr} for each of the slags (Table V). D_i values for Ca and Si were not calculated since the concentrations of these elements in the M_3O_5 solid solutions were not accurately measured. Data for silicate phases with different compositions in the same slag were used to calculate average values for the D_i. Where data for silica-poor glass were not available, inequalities were used to indicate the bias (samples B4, E2, F3 and G3).

Elements may be classified according to their partition coefficients:

- Silicon, calcium (and thorium) have large partition coefficients, which means that they are strongly concentrated in the silicate phases. Manganese also prefers silicate phases but its partition coefficient is considerably smaller (about 10)
- Iron, magnesium, chromium and aluminium have distribution coefficients that are around unity, which

Table V

Average distribution coefficients (silicate-oxide) for Mn, Mg, Al, Fe, Ti and Cr for each of the slags (the range over which D_i varies is reflected as an uncertainty)

	A1	A6	A12	B4	BB1	BBB1	E2	F3	G3	H4
D_{Mn}	9.7 ± 2.3	7.6 ± 4.7	7.6 ± 3.9	> 3.6	8.5 ± 1.4	9.9 ± 1.8	> 2.3	> 4.5	> 2.4	7.8 ± 3.5
D_{Mg}	0.6 ± 0.1	0.4 ± 0.2	0.5 ± 0.2	> 0.3	0.9 ± 0.1	1.1 ± 0.2	> 0.2	> 0.1	> 0.1	0.4 ± 0.2
D_{Al}	3.4 ± 0.2	3.2 ± 0.7	3.5 ± 0.7	~ 2.8	3.3 ± 0.2	3.7 ± 0.0	~ 3.8	~ 3.5	~ 3.6	3.5 ± 0.4
D_{Fe}	0.8 ± 0.2	1.0 ± 0.7	0.9 ± 0.4	> 0.4	1.1 ± 0.4	0.8 ± 0.3	0.7 ± 0.4	> 0.5	> 0.3	0.7 ± 0.3
D_{Ti}	0.09 ± 0.01	0.08 ± 0.05	0.09 ± 0.00	~ 0.10	0.06 ± 0.01	0.11 ± 0.04	0.10 ± 0.03	~ 0.08	~ 0.07	0.12 ± 0.05
D_{Cr}	0.5 ± 0.1	0.2 ± 0.1	0.2 ± 0.0	> 0.3	0.4 ± 0.1	0.7 ± 0.2	> 0.1	> 0.2	> 0.1	0.4 ± 0.3

Distribution coefficients for B4, E2, F3 and G3 are not well constrained due to a lack of analytical data. Symbols are used to indicate the bias resulting from the lack of data.

Table VI

Calculated mass-percentage of silicate and oxide phases in each slag and the calculated thorium distribution

	A1	A6	A12	B4	BB1	BBB1	E2	F3*	G3	H4
% silicate phases	5.1 ± 2.1	4.8 ± 1.8	5.5 ± 2.7	5.9 ± 2.8	7.6 ± 2.7	7.8 ± 2.9	5.2 ± 2.2	6.5 ± 6.2	5.1 ± 4.0	5.4 ± 2.8
% oxide phases	94.9 ± 2.1	95.2 ± 1.8	94.5 ± 2.7	94.1 ± 2.8	92.4 ± 2.7	92.2 ± 2.9	94.8 ± 2.2	93.5 ± 6.2	94.9 ± 4.0	94.6 ± 2.8
Bulk Th (ppm)	139	182	161	177	203	173	336	220	177	50
Th concentration in silicates (ppm)	3696 ± 757	3872 ± 797	4459 ± 835		2992 ± 373	2596 ± 249	6160 ± 2330	4500		836 ± 670
Th in slag contained in silicates (mgTh/g slag)	188 ± 86	185 ± 79	245 ± 128		227 ± 85	202 ± 77	320 ± 182	292 ± 278		45 ± 42
Th in slag contained in oxides (mgTh/g slag)	< 37	< 76	< 44		< 61	< 48	< 198	< 206		< 47
Th concentration in oxides (ppm)	< 39	< 80	< 46		< 65	< 52	< 208	< 220		< 50
DTh	> 95	> 48	> 97		> 46	> 50	> 30	> 20		> 17

'Bulk Th' is the bulk Th content of the slag (from Table I)
'Th concentration in silicates' is the average Th concentration in silicate phases determined by microprobe
'Th in slag contained in silicates' is the amount of thorium contained in the silicate phases in the slag
'Th in slag contained in oxides' is the amount of thorium contained in the oxide phases in the slag
'Th conc. in oxides' indicates the maximum Th concentration in oxide phases calculated from the Th distribution
D_{Th} is the minimum value of the silicate-oxide distribution coefficient for Th
The Th distribution in E2 and H4 are subject to large uncertainties due to the large difference in the Th content of the silicate phases
Calculations are based on semi-quantitative PIXE data

means that they are evenly distributed between silicate and oxide phases

- Titanium has a very small distribution coefficient (~ 1/100), which means that it is strongly concentrated in oxide phases.

The distribution coefficients indicate how the removal of silicate phases from the slag will affect the composition of the oxide residue. Elements that preferentially partition to silicate phases ($D_i > 1$) will be depleted in the residue (i.e., the composition of the residual oxide slag will be upgraded through the removal of these elements), whereas elements for which $D_i < 1$ will be enriched in the residue (providing insoluble oxides do not precipitate during leaching). Leaching of silicate phases should therefore result in a decrease in the concentrations of SiO_2, CaO and Th (to a lesser extent also MnO), and an increase in the concentration of TiO_2 in the oxide residues. The concentrations of FeO, MgO, Al_2O_3 and Cr_2O_3 in the oxide residues will not be significantly affected by the removal of silicate phases.

The chemical behaviour of thorium in high-titania slag

Distribution of thorium between silicate and oxide-phases

Although the distribution coefficient could not be measured directly, it is possible to constrain the distribution of thorium through calculation.

First, the weight fractions of silicate and oxide phases in each slag are calculated. The average concentrations of MnO, SiO_2, TiO_2 and CaO in silicate and oxide phases are used for this purpose because of the magnitudes of the silicate-oxide distribution coefficients of these elements. Next, the amount of thorium reporting to silicate phases (in μg/g slag) is calculated from the weight percentage silicate phases in the slag and the average thorium concentration in the silicate phases. Standard error-propagation techniques are used to calculate the uncertainties in these quantities. Within the

uncertainty of the data, the amount of thorium reporting to the silicate phases is enough to account for the mean total thorium content of the slags and, as a result, only a maximum value for the amount of thorium reporting to oxide phases can be calculated (this being the difference between the total thorium content of the slag and the amount of thorium present in silicate phases—taking the uncertainties in the data into account). Following the calculation of a maximum value for the amount of thorium present in oxide phase, a minimum value for the thorium distribution coefficient can be calculated. Results of these calculations are reported in Table VI.

The calculation is complicated by the large difference in thorium content of the silica-rich and silica-poor glasses. In the case of slags B4 and G3, calculation of the distribution coefficient was not attempted because of a lack of data for the thorium-rich, silica-poor, glass. Although WDS data are not available for F3 either, semi-quantitative PIXE analyses for this sample are consistent with a value for the thorium distribution coefficient of at least 20. Consistently large distribution coefficients for thorium lead to an important conclusion:

- The removal of silicate phases will also remove the bulk of the thorium and cause a significant decrease in the thorium content of the oxide residue.

It is informative to consider the significance of a large distribution coefficient for thorium between silicate and oxide phases. Consider a slag containing 5 wt% silicate phases and a bulk Th content of 200 ppm. Assuming $D_{Th}^{Silicate-oxide} = 100$, it follows that the Th concentration in the silicate and oxide phases will be 3360 ppm and 33.6 ppm respectively. Therefore, if the silicate phases could be fully leached from the slag, it should be possible to reduce the thorium content by at least 84%.

A large value for D_{Th} is consistent with the general incompatible behaviour of thorium during the crystallization of magma with different compositions[5] (an element is said to be 'incompatible' if it is concentrated in the residual melt once different oxide and silicate minerals start to crystallize during cooling). Unfortunately, there are no data for D_{Th} between silicate melt and M_3O_5 oxide phases in the geological literature that could be used for comparison with the results of this study.

Discussion

The silicate phases in the slags were previously identified as quenched silicate melt (i.e., glass). It is therefore relevant to consider the chemistry of thorium in silicate melts as it may suggest options for optimizing the amount of thorium reporting to the silicate melt phases during smelting. The most stable oxidation state for thorium is +4; with respect to thorium metal, it is also one of the most stable oxides. The stability of ThO_2 relative to Th plus oxygen is evident from the Gibbs free energy of formation of ThO_2; approximately -870 KJ.mol^{-1} at 1900 K (1627°C). By comparison, the Gibbs free energy of formation of TiO_2 (relative to Ti and O_2) at 1900 K is about -603 KJ.mol^{-1}. In terms of oxygen partial pressure (PO_2) it means that ThO_2 will form when the PO_2 exceeds $10^{-23.8}$ bar, while TiO_2 will (form from Ti and O_2) when the PO_2 exceeds $10^{-16.5}$ bar. A practical implication of this result is that metallic thorium will not form during smelting and the Th content of the pig iron will be negligible.

It is not known what the effective oxygen partial pressure during smelting is; it will also be different for the different slags (hence the differences in Fe/Ti ratio of the slags). Phase-chemically, the composition of the M_3O_5 phases that crystallize from iron-titanium oxide slag may effectively be described in terms of the $FeTi_2O_5$-Ti_3O_5 solid solution series. The activity of Ti_3O_5 in the slag increases with increasing grade, and when all the Fe^{2+} is reduced to metallic iron (Fe0) the activity of Ti_3O_5 is almost unity. An indication of the minimum oxygen partial pressure during smelting may therefore be obtained from the equilibrium between solid Ti_3O_5 and TiO_2 (rutile):

$$Ti_3O_5 + \tfrac{1}{2}O_2 = 3TiO_2 \qquad [3]$$

Using thermodynamic data of Barin[6], the equilibrium oxygen partial pressure for reaction 1 at 1900 K is $10^{-9.3}$ bar (this is about 1.3 $\log_{10}$-units more reducing than the Fe-FeO buffer). The oxidation of solid Ti_4O_7 to TiO_2 (rutile) at 1900 K takes place at a very similar oxygen partial pressure ($10^{-9.2}$ bar), indicating that solid Ti^{3+}-bearing oxide phases are stabilized at oxygen partial pressures approximately 7 log10-units more oxidizing than the Ti-TiO_2 buffer. Assuming similar behaviour in the thorium-oxygen system, the formation of Th^{3+}-bearing oxide phases at 1900 K might be expected at oxygen partial pressures of about 10^{-17} bar. This is about 8 log10-units more reducing than the minimum oxygen partial pressure likely to be attained during smelting ($10^{-9.3}$ bar). Although these calculations are not directly applicable to the oxidation state of multi valent cations in melt phases, the data suggest that the ratio of Th^{3+} to Th^{4+} is likely to be very low, even under the most reducing conditions expected during smelting.

The structural environment around Th^{4+} in silicate glasses containing between 1% and 3% (by weight) Th^{4+} was investigated by Farges[4] using extended X-ray absorption fine structure (EXAFS) spectroscopy. Several conclusions from the work by Farges[4] are directly applicable to current problem:

- Th^{4+} is mainly six co-ordinated by oxygen with a mean bond length, $\langle^{VI}$Th-O.$\rangle$ of about 2.3 Å. Eight-co-ordinated Th^{4+} $\langle^{VIII}$Th-O$\rangle$ ~ 2.4 Å) is present at high thorium concentration levels (3%) and/or when polymerization increases. Mean metal-oxygen bond lengths for the two six-co-ordinated cation sites (M_1 and M_2) in orthorhombic Ti_3O_5-rich solid solutions $\langle^{VI}M_1$-O$\rangle$ and $\langle^{VI}M_2$-O$\rangle$ are approximately 2.04 Å and 2.01 Å, respectively[4]. The much shorter metal-oxygen bond lengths in Ti_3O_5-rich solid solutions mean that thorium is unlikely to partition into oxide phases crystallizing from the slag during cooling
- The amount of six-co-ordinated Th^{4+} ($^{VI}Th^{4+}$) increases in the presence of major quantities of alkali cations such as Na^+ and K^+. Should the addition of such fluxes be practical, it will facilitate the collection of thorium by

silicate melt phases during smelting

- The bond strength around six-co-ordinated Th^{4+} in silicate melt or glass is high relative to that in Th-bearing minerals such as ThO_2 and $ThSiO_4$. This explains in part why these phases are not observed in the slags, even at high bulk thorium concentration levels (> 300 ppm)
- Increasing polymerization of the silicate glass or melt (high concentrations of SiO_2), will favour higher co-ordinations around Th^{4+} due to a lack of non-bridging oxygens (NBOs) to which thorium preferentially bonds. This explains why the silica-rich glass phase contains less thorium than the co-existing, low silica, glass phase in the slags.

To summarize: data on the chemical behaviour of thorium in silicate melts and glasses support the mass-balance calculations according to which the amount of thorium in silicate glass phases is sufficient to account for the total thorium content of the slags.

Summary

Elements with a large ionic radius preferentially partition to the immiscible silicate melt that forms during smelting. These elements include thorium (which is present in such large quantities that its concentration in silicate phases could be measured by electron microprobe), zirconium, barium, lanthanum, niobium, cerium (the distribution of these elements was determined by PIXE), and possibly also the radioactive daughter elements of the thorium- and uranium-decay series.

Mass balance calculations suggest that the thorium content of the silicate phases is high enough to account for the total thorium content of the slags. This is also reflected by the silicate-oxide distribution coefficients for Th that are overwhelmingly in favour of the silicate phases. Depending on the total silica content, silicate phases constitute approximately 4 to 8 weight per cent of the slags that were selected for test work.

Spectroscopic data in the literature are consistent with the partitioning of thorium into depolymerized (low-silica) glasses and melts relative to crystalline phases and more polymerized glasses and melts. These results are in agreement with the observations of this study and confirm that silicate phases contain most of the thorium present in the slag.

In principle, the radioactivity levels of high titania slag can be lowered by the removal (physical or chemical) of silicate phases from the slag. Disposal of the radioactive, silicate fraction will be onerous and the economics of such a step are questionable.

References

1. RGC Mineral Sands Ltd., S.A. Patent no. 93/5474, 29 July 1993.
2. Bessinger, D., Du Plooy, H., Pistorius, P.C., and Visser, C. Characteristics of some high titania slags. *Heavy Minerals*. R.E. Robinson. (ed.) Johannesburg, South African Institute of Mining and Metallurgy, 1997. pp. 151–156.
3. Eller, P.G., Jarvinen, G.D., Purson, R.A., Penneman, R.R., Lytle, F.W., and Greegor, R.B. Actinide abundances in borosilicate glass. *Radiochimica Acta*, vol. 39, 1985. pp. 17–22
4. Farges, F. Structural environment around Th^{4+} in silicate glasses: Implications for the geochemistry of incompatible M^{4+} elements. *Geochimica et Cosmochimica Acta*, vol. 55, 1991. pp. 3303–3319.
5. Mahood, G.A. and Hildreth, W. Large partition coefficients for trace elements in high silica rhyolites. *Geochimica et Cosmochimica Acta*, vol. 47, 1983. pp. 11–30.
6. Barin, I. *Thermochemical Data of Pure Substances, Parts I and II*. VCH Verlagsgesellschaft. 1989. ◆